VIP *The following Communications have been judged by at least two referees to be "very important papers" and will be published online at www.angewandte.org soon:*

C. Schäffer, A. Merca, H. Bögge, A. M. Todea, M. L. Kistler, T. Liu, R. Thouvenot, P. Gouzerh, A. Müller**
Unprecedented and Differently Applicable Pentagonal Units in a Dynamic Library: A Keplerate of the Type $\{(\mathrm{W})\mathrm{W}_5\}_{12}\{\mathrm{Mo}_2\}_{30}$

*S. W. Hong, M. Byun, Z. Lin**
Robust Self-Assembly of Highly Ordered Complex Structures by Controlled Evaporation of Confined Microfluids

L. Catala, D. Brinzei, Y. Prado, A. Gloter, O. Stéphan, G. Rogez, T. Mallah**
Core–Multishell Magnetic Coordination Nanoparticles: Towards Multifunctionality at the Nanoscale

*D. Morton, S. Leach, C. Cordier, S. Warriner, A. Nelson**
Synthesis of Natural-Product-Like Molecules with over Eighty Distinct Scaffolds

*O. Vendrell, F. Gatti, H.-D. Meyer**
Strong Isotope Effects in the Infrared Spectrum of the Zundel Cation

*W. M. Czaplik, M. Mayer, A. Jacobi von Wangelin**
Domino Iron Catalysis: Direct Aryl–Alkyl Cross-Coupling

Z. You, A. H. Hoveyda, M. L. Snapper**
Catalytic Enantioselective Silylation of Acyclic and Cyclic Triols and Application to Total Syntheses of Cleroindicins D, F, and C

*K. Tedsree, A. T. Kong, S. C. Tsang**
Formate as a Surface Probe for Ru Nanoparticles in Liquid ^{13}C NMR Spectroscopy

*A. Asati, S. Santra, C. Kaittanis, S. Nath, J M. Perez**
Oxidase Activity of Polymer-Coated Cerium Oxide Nanoparticles

News

Highlights

C–C Coupling

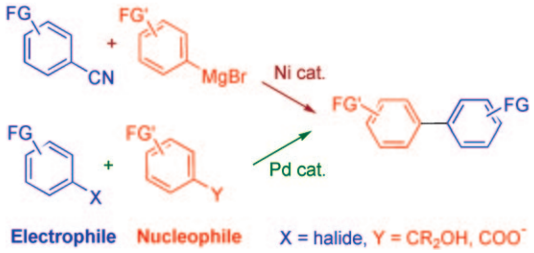

No loss, no gain: In the synthesis of biaryls either the electrophilic or nucleophilic partner can be replaced by a substrate with a carbon-based leaving group (see scheme). Whereas replacing the electrophilic unit is not worthwhile, the use of nucleophiles with a C-based leaving group has decisive advantages.

Contents

Essays

Chemical concepts and quantum mechanics: Heuristic concepts are indispensable tools to give the almost boundless body of knowledge in chemistry an ordered structure and to present it didactically. Many of these concepts were developed without a full understanding of their physical backgrounds. Pulling together results from quantum chemical calculations and conceptual quantities is not always straightforward and requires close consideration of the definition of the quantity in question.

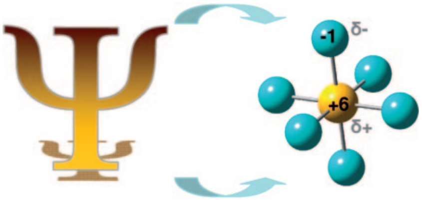

Reviews

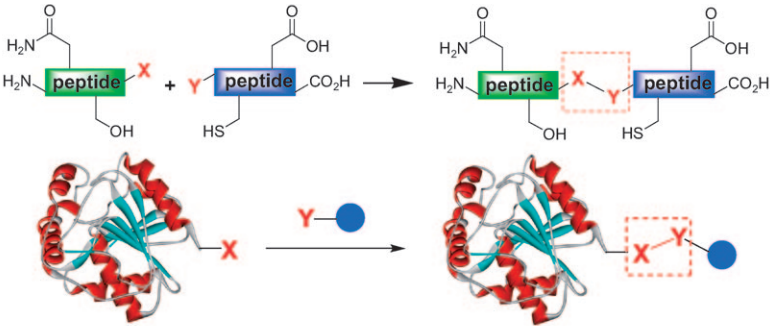

Selectivity is the key! Chemoselective ligation and modification strategies are important methods for linking synthetic or recombinant unprotected peptides to generate large polypeptides (see scheme). Recent developments in this research area have led to numerous applications in the semisynthesis and total synthesis of proteins.

Communications

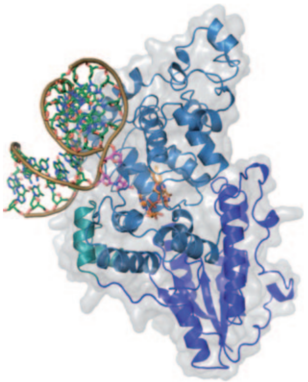

Before and after: Crystal structures of the DNA (6-4) photolyase from *D. melanogaster*—one structure in complex with DNA containing a (6-4) lesion (see picture) and one in which the lesion has been repaired—provide new insight into lesion recognition and repair. The proposed mechanism for light-induced, electron-transfer-based repair of the (6-4) lesion does not proceed via an oxetane intermediate.

For the USA and Canada:
ANGEWANDTE CHEMIE International Edition (ISSN 1433-7851) is published weekly by Wiley-VCH, PO Box 191161, 69451 Weinheim, Germany. Air freight and mailing in the USA by Publications Expediting Inc., 200 Meacham Ave., Elmont, NY 11003. Periodicals postage paid at Jamaica, NY 11431. US POSTMASTER: send address changes to *Angewandte Chemie*, Wiley-VCH, 111 River Street, Hoboken, NJ 07030. Annual subscription price for institutions: US$ 7225/6568 (valid for print and electronic / print or electronic delivery); for individuals who are personal members of a national chemical society prices are available on request. Postage and handling charges included. All prices are subject to local VAT/ sales tax.

Marine Natural Products

C. Hamel, E. V. Prusov,
J. Gertsch, W. B. Schweizer,
K.-H. Altmann* ________ 10081 – 10085

Total Synthesis of the Marine Diterpenoid Blumiolide C

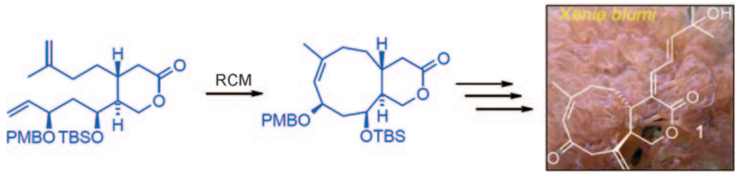

First bloom: The total synthesis of the cytotoxic marine natural product blumiolide C (**1**) features a ring-closing metathesis (RCM) for the closure of a nine-membered ring to give the *trans*-bicyclo[7.4.0]oxatridecene core (see scheme; PMB = *para*-methoxybenzyl, TBS = *tert*-butyldimethylsilyl). Attachment of the side chain at C4 of the bicyclic core was achieved in a highly stereoselective manner and excellent yield through an aldol reaction/elimination sequence.

Applied Biocatalysis

C. Goedl, T. Sawangwan, M. Mueller,
A. Schwarz, B. Nidetzky* 10086 – 10089

A High-Yielding Biocatalytic Process for the Production of 2-*O*-(α-D-glucopyranosyl)-*sn*-glycerol, a Natural Osmolyte and Useful Moisturizing Ingredient

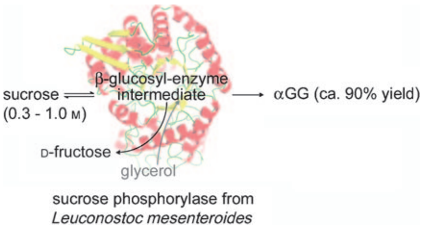

Fit for industry: Stereochemically pure 2-*O*-(α-D-glucopyranosyl)-*sn*-glycerol (αGG) was obtained in high yield from an efficient and selective biocatalytic process (see schematic outline). The sucrose phosphorylase catalyzed transfer of a glucosyl group from sucrose to glycerol unites the main advantages of transglycosidases, glycosyltransferases, and glycosynthases for glycoside synthesis and provides access to αGG as an industrial chemical.

Asymmetric Synthesis

M. Rueping,*
A. P. Antonchick ________ 10090 – 10093

Catalytic Asymmetric Aminoallylation of Aldehydes: A Catalytic Enantioselective Aza-Cope Rearrangement

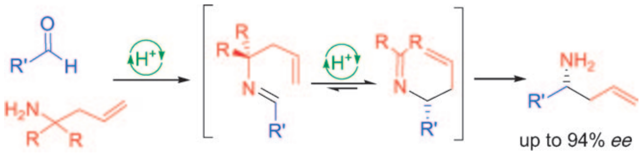

A condensation–rearrangement sequence forms the basis of a high-yielding route to chiral homoallylic amines from readily accessible aldehydes (see scheme). This transformation is both the first enantioselective Brønsted acid catalyzed sigmatropic rearrangement and the first example of a catalytic asymmetric aza-Cope rearrangement.

Cluster Growth

M. Busker, T. Häber, M. Nispel,
K. Kleinermanns* ________ 10094 – 10097

Isomer-Selective Vibrational Spectroscopy of Benzene–Acetylene Aggregates: Comparison with the Structure of the Benzene–Acetylene Cocrystal

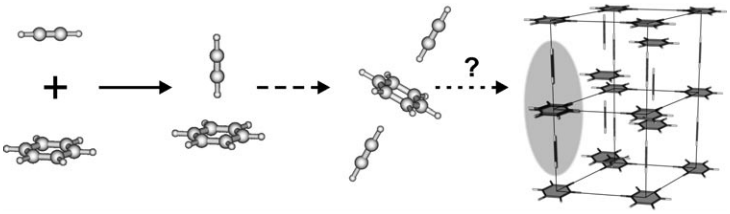

Crystallization seeds in supersonic jets? T-shaped structures dominate the isomer-selective IR–UV double-resonance spectra of benzene–acetylene clusters in supersonic jets. The double T-shaped motif is also present in the 1:1 cocrystal (see picture).

Spin-Crossover Complexes

B. Weber,* W. Bauer,
J. Obel ———— 10098 – 10101

An Iron(II) Spin-Crossover Complex with a 70 K Wide Thermal Hysteresis Loop

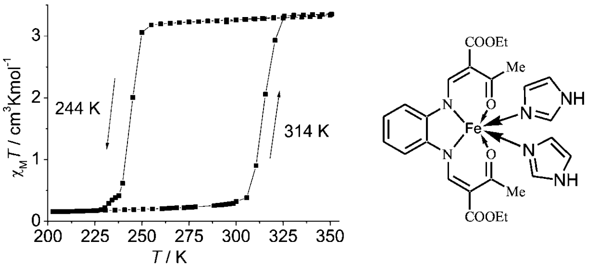

Going loopy: A new iron(II) spin-crossover complex displays a 70 K wide thermal hysteresis loop, which can be explained by an intermolecular 2D network of hydrogen bonds. This is the first example of a spin-crossover complex with wide hysteresis arising from a hydrogen-bond network; it displays the widest hysteresis to date for a structurally characterized complex.

Delocalized Bonding

J. S. Pap, S. DeBeer George,
J. F. Berry* ———— 10102 – 10105

Delocalized Metal–Metal and Metal–Ligand Multiple Bonding in a Linear Ru–Ru≡N Unit: Elongation of a Traditionally Short Ru≡N Bond

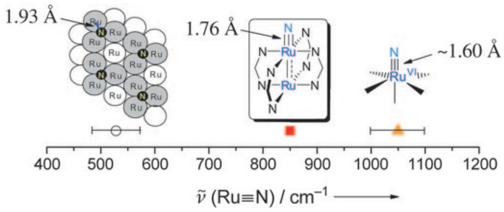

Long-distance Ru≡N-ning: The depicted metal–metal-bonded diruthenium(III,IV) complex binds a terminal nitrido ligand with delocalized Ru–Ru≡N multiple bonding. The Ru≡N bond (1.76 Å) is remarkably long in comparison with mononuclear ruthenium nitrido complexes and has been shown by vibrational spectroscopy data to be exceptionally weak.

Carbocations

P. Rubenbauer, E. Herdtweck, T. Strassner,
T. Bach* ———— 10106 – 10109

Bi(OTf)$_3$-Catalyzed Diastereoselective S$_N$1-Type Reactions of Chiral Propargylic Acetates

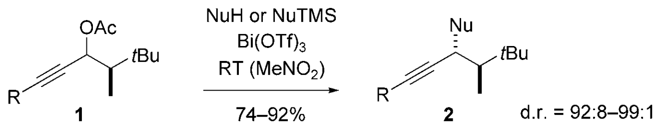

Stereoelectronic factors are apparently responsible for the high selectivity observed in the title S$_N$1-type reaction of acetates **1** in favor of the *anti* products **2**. The preferred conformation of the intermediate propargylic cations would lead to the *syn* product; however, a second conformation exists, in which the *tert*-butyl group adopts an antiperiplanar orientation with respect to the incoming nucleophile. Tf = trifluoromethanesulfonyl, TMS = trimethylsilyl.

Homogeneous Catalysis

Y. Zou, D. Garayalde, Q. Wang,*
C. Nevado,* A. Goeke* —— 10110 – 10113

Gold-Catalyzed Cycloisomerization of Cyclopropyl Alkynyl Acetates: A Versatile Approach to 5-, 6-, and 7-Membered Carbocycles

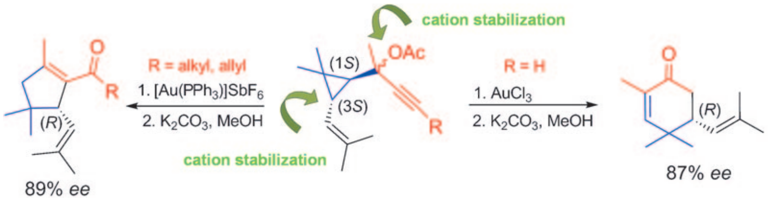

Nonclassical chirality transfer? Depending on the substitution pattern of propargyl acetates, a gold-catalyzed homologous Rautenstrauch reaction generates either 5- or 6-membered ring systems (see scheme). The stabilization of cationic intermediates is crucial for this reaction to succeed. The underlying principle for the good chirality transfer observed could be gold-stabilized nonclassical carbocations having configurational stability.

Chalcogenocarboxylic Acids

J. A. Gómez Castaño, R. M. Romano,
H. Beckers, H. Willner, R. Boese,
C. O. Della Védova* ______ **10114 – 10118**

Selenoacetic Acid, $CH_3C(O)SeH$: Preparation, Characterization, and Conformational Properties

The elusive congener: Selenoacetic acid is prepared for the first time by warming a mixture of acetic acid and Woollins' reagent ($Ph_2P_2Se_4$) under moisture- and air-free conditions. In the crystal structure of $CH_3C(O)SeH$, amongst the possible *syn* (top) and *anti* (bottom) conformations, the *anti* is preferred (see picture; C gray, H white, O red, Se magenta).

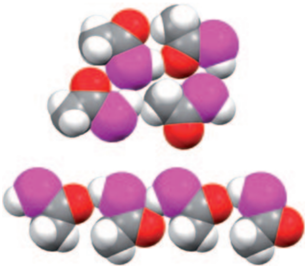

Phase Transitions

J. Zhang, B. Han,* W. Li, Y. Zhao,
M. Hou ________________ **10119 – 10123**

Reversible Switching of Lamellar Liquid Crystals into Micellar Solutions using CO_2

Changing under pressure: Compressed CO_2 can switch the surfactant sodium bis-2-ethylhexylsulfosuccinate/water system between a lamellar liquid crystal (L_α) phase and a micellar solution (L_1) reversibly at ambient temperature. Applications of this simple, clean, and energy-efficient process in material synthesis are explored, along with a possible mechanism for the phase-transition phenomenon.

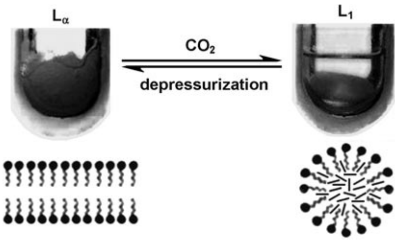

Bond Activation

B.-J. Li, Y.-Z. Li, X.-Y. Lu, J. Liu, B.-T. Guan,
Z.-J. Shi* ________________ **10124 – 10127**

Cross-Coupling of Aryl/Alkenyl Pivalates with Organozinc Reagents through Nickel-Catalyzed C–O Bond Activation under Mild Reaction Conditions

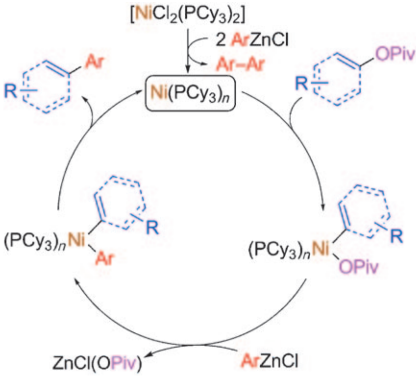

Finding the right partner: The catalyst system $[NiCl_2(PCy_3)_2]$ mediates the title transformation with high efficiency and allows aryl–aryl and vinyl–aryl coupling to proceed. The first example of catalytic cross-coupling using the pivalates and organozinc reagents is described (see scheme; Cy = cyclohexyl, piv = pivalate).

Analytical Methods

N. C. Jeong, J. S. Lee, E. L. Tae, Y. J. Lee,
K. B. Yoon* ______________ **10128 – 10132**

Acidity Scale for Metal Oxides and Sanderson's Electronegativities of Lanthanide Elements

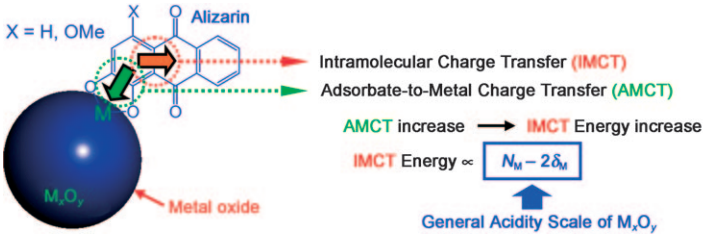

Acid trip: A general scale that compares the acidities of metal oxides and sulfides quantitatively is presented, along with Sanderson's electronegativity values of lanthanides.

Asymmetric Catalysis

W.-J. Lu, Y.-W. Chen,
X.-L. Hou* ———— **10133 – 10136**

Iridium-Catalyzed Highly Enantioselective Hydrogenation of the C=C Bond of α, β-Unsaturated Ketones

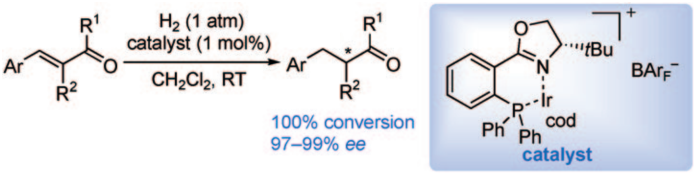

A fine selection: The installation of chiral centers at the α position of ketones is achieved with excellent enantioselectivity by means of iridium-catalyzed asymmetric hydrogenation of α,β-unsaturated ketones under mild conditions. The catalyst incorporates a phosphinooxazoline (PHOX)-based ligand, which exhibits high levels of asymmetric induction (see scheme; BAr_F^- = tetrakis[3,5-bis(trifluoromethyl)phenyl]borate; cod = cycloocta-diene).

Natural Product Synthesis

C. Bressy, J.-P. Vors, S. Hillebrand,
S. Arseniyadis, J. Cossy* ‗ **10137 – 10140**

Asymmetric Total Synthesis of the Immunosuppressant (−)-Pironetin

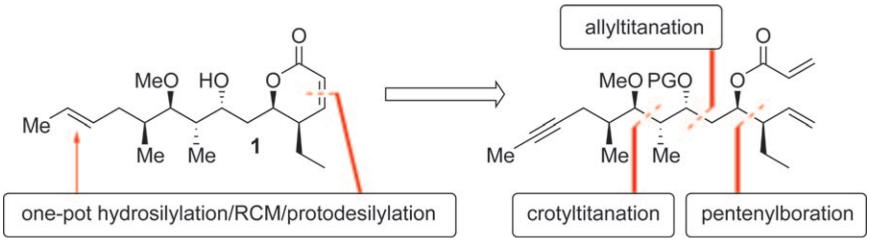

A short, enantioselective total synthesis of the title compound **1** is described. The 14-step synthesis features a highly stereoselective Brown-type pentenylation and a one-pot hydrosilylation/ring-closing metathesis (RCM)/protodesilylation sequence as the key steps. PG = protecting group.

Radiolabeling

M. Winkler,* J. Domarkas, L. F. Schweiger,
D. O'Hagan* ———— **10141 – 10143**

Fluorinase-Coupled Base Swaps: Synthesis of $[^{18}F]$-5′-Deoxy-5′-fluorouridines

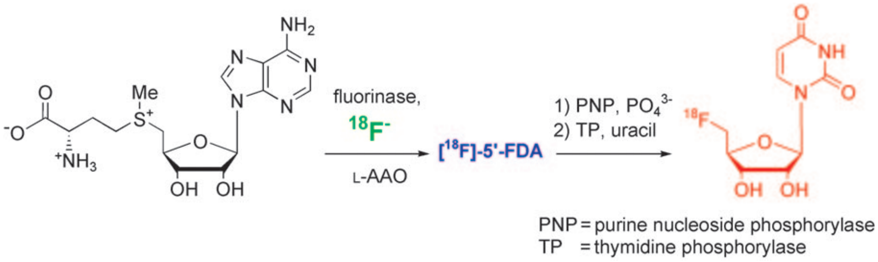

Making F-ases: One-pot fluorination/base-swap biotransformations were developed by coupling the fluorinase enzyme to nucleoside phosphorylases to generate 5′-deoxy-5′-fluoronucleosides (FDAs). These biotransformations are amenable to radiolabeling syntheses starting from $[^{18}F]$fluoride ion, as exemplified by the synthesis of $[^{18}F]$-5′-deoxy-5′-fluorouridines (see scheme), and demonstrate a new application of fluorinase as a catalyst for ^{18}F–C bond formation.

Spin Crossover

J. Li, R. L. Lord, B. C. Noll,
M.-H. Baik, C. E. Schulz,
W. R. Scheidt* ———— **10144 – 10146**

Cyanide: A Strong-Field Ligand for Ferrohemes and Hemoproteins?

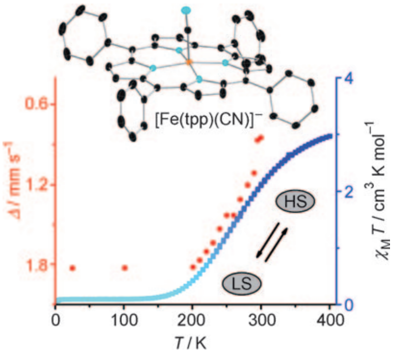

A CN weakling? The cyanide ligand in the five-coordinate iron(II) porphyrinate complex $[Fe(tpp)(CN)]^-$ (tpp = tetraphenylporphinato) is not a sufficiently strong-field ligand to cause the complex to be in the low-spin state under all conditions. Rather, the complex displays a reversible low-spin (LS) to high-spin (HS) crossover with no hysteresis.

Cluster Compounds

M. P. Coles,* S. M. El-Hamruni,
J. D. Smith,
P. B. Hitchcock ________ 10147 – 10150

An Organozinc Hydride Cluster: An Encapsulated Tetrahydrozincate?

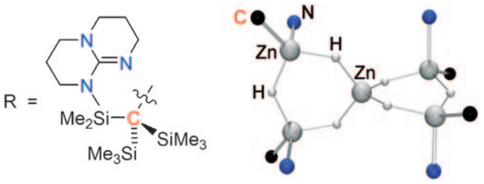

Zinc for a minute: The reaction of the alkylzinc bromide $[Zn\{C(SiMe_3)_2(SiMe_2hpp)\}]Br$ (see structure) with an excess of sodium hydride gives good yields of an unusual zinc hydride cluster, in which five zinc atoms are linked by (μ-H) bridges, to form a spirocyclic $[Zn\{(\mu\text{-}H)Zn\}_4(\mu\text{-}H)_2]^{4+}$ array, in which two six-membered $\{Zn(\mu\text{-}H)\}_3$-rings are fused at one zinc center.

Anode Materials

H. Kim, B. Han, J. Choo,
J. Cho* ________ 10151 – 10154

Three-Dimensional Porous Silicon Particles for Use in High-Performance Lithium Secondary Batteries

Particle-larly good! Thermal annealing and etching of physical composite butyl-capped Si gels and SiO_2 nanoparticles at 900 °C under an Ar atmosphere is a versatile method for the formation of 3D porous bulk Si particles (see picture). Complete etching of the SiO_2 from the SiO_2/carbon-coated Si (c-Si) composite results in the retention of the remaining c-Si as a highly porous but interconnected structure, which preserves the starting morphology.

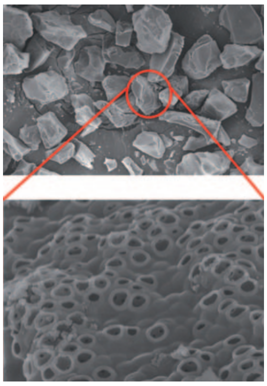

Asymmetric Synthesis

D. Marcoux,
A. B. Charette* ________ 10155 – 10158

trans-Directing Ability of Amide Groups in Cyclopropanation: Application to the Asymmetric Cyclopropanation of Alkenes with Diazo Reagents Bearing Two Carboxy Groups

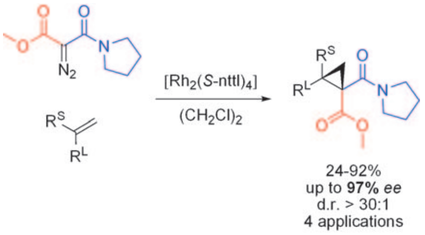

Highly stereoselective: A highly enantioselective (up to 97% *ee*) and diastereoselective (> 30:1 d.r.) Rh^{II}-catalyzed cyclopropanation of alkenes using a diazo reagent bearing two carboxy groups is described. This new methodology exploits the powerful *trans*-directing ability of amides to improve enantiocontrol. Mono- and disubstituted olefins are cyclopropanated in good yields. nttl = *N*-1,8-naphthoyl-*tert*-leucine.

Heterometallic Complexes

H. Kameo, Y. Nakajima,
H. Suzuki* ________ 10159 – 10162

Drastic Acceleration of Phosphine/Phosphite Incorporation into a Tetrahydrido Ruthenium/Osmium Complex, and One-way Ruthenium to Osmium Migration of a Phosphorus Ligand

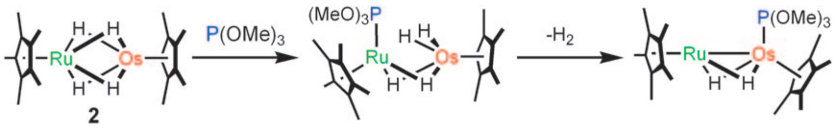

Unequal partners: Reactions of complexes of the form $[Cp^*M(\mu\text{-}H)_4M'Cp^*]$ (**1**: M = M′ = Ru; **2**: M = Ru, M′ = Os; **3**: M = M′ = Os) with $P(OMe)_3$ provide evidence of kinetic and thermodynamic heterometallic effects. Heterometallic complex **2** induces selective addition of $P(OMe)_3$ to the Ru center in an accelerated reaction. Moreover, the incorporated $P(OMe)_3$ migrates unidirectionally from Ru to Os owing to the formation of a strong Os–P bond.

PtBi Catalysts

S. Uhm, H. J. Lee, Y. Kwon,
J. Lee* ———— 10163 – 10166

A Stable and Cost-Effective Anode Catalyst Structure for Formic Acid Fuel Cells

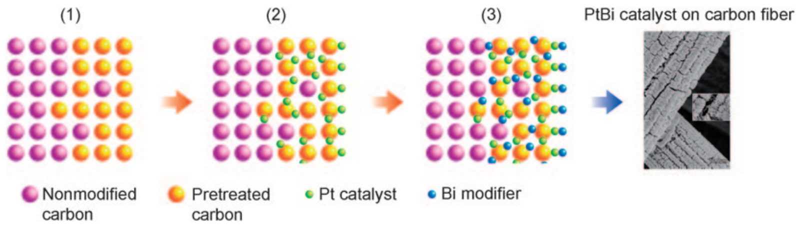

Cheap and stable: A PtBi catalyst was fabricated in three consecutive electrochemical steps (see picture): electrochemical oxidation of carbon paper to form an adequate catalyst support (1), Pt electrodeposition (2), and underpotential deposition of Bi onto the as-prepared Pt (3). This process resulted in a well-dispersed and thin catalyst layer as well as a significantly enhanced power performance with a Pt loading of only 0.5 mg cm^{-2}.

Drug Detection

VIP

P. Hazarika, S. M. Jickells, K. Wolff,
D. A. Russell* ———— 10167 – 10170

Imaging of Latent Fingerprints through the Detection of Drugs and Metabolites

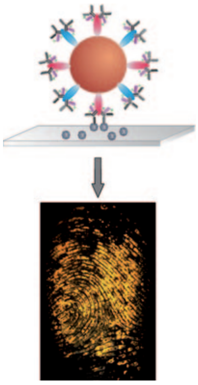

Dusting for prints: Antibody–magnetic-particle conjugates comprise protein-coated magnetic particles labeled with dye-tagged fragments (see picture). These particles bind to drugs and drug metabolites such as methadone and benzoylecgonine that are deposited within a latent fingerprint. The conjugates provide a means to image the fingerprint and enable the identification of an individual whilst simultaneously providing evidence of drug usage.

Amphiphilic Particles

L. Cheng, G. Zhang, L. Zhu,* D. Chen,*
M. Jiang ———— 10171 – 10174

Nanoscale Tubular and Sheetlike Superstructures from Hierarchical Self-Assembly of Polymeric Janus Particles

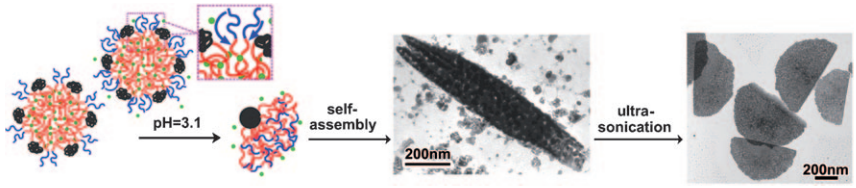

Two faces: Starting from mixed shell micelles, amphiphilic Janus particles with opposite hydrophobic and hydrophilic complex sides were obtained by intramicellar complexation between the mixed shell and the core at pH 3.1 (see picture). Hierarchical self-assembly of these Janus particles in water resulted in a nanoscale tubular superstructure, which was then converted into regular nanosheets upon ultrasonication.

Dendrimers

T. M. Figueira-Duarte, S. C. Simon,
M. Wagner, S. I. Druzhinin,
K. A. Zachariasse,*
K. Müllen* ———— 10175 – 10178

Polypyrene Dendrimers

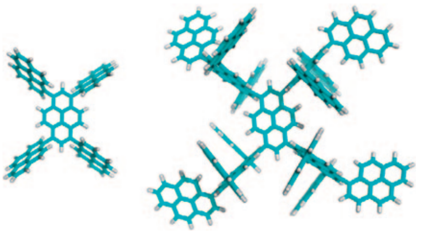

Branching out: Stiff, aromatic dendrimers made up of five and seventeen pyrene units, respectively, are synthesized, characterized, and compared with two model compounds. The rigid and strongly twisted structure allows a precise spatial arrangement in which each unit is a chromophore. The high extinction coefficients and fluorescence quantum yields make these dendrimers attractive candidates for use as fluorescence labels.

Protein Macrocyclization

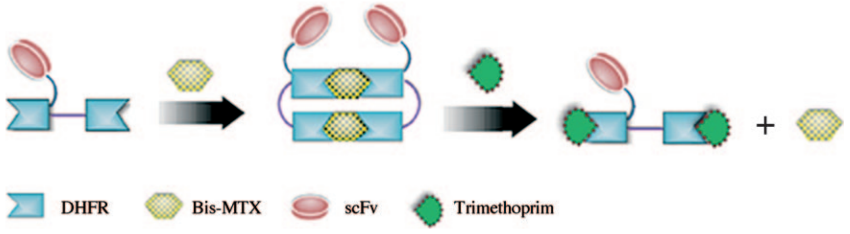

Getting together and breaking up: Circular arrays of recombinant antibodies can be produced reversibly by chemically controlled protein macrocyclization. In the presence of bismethotrexate (bis-MTX), dimeric dihydrofolate reductase fusion protein (DHFR) with an anti-CD3 single-chain variable region (scFv) self-assembled spontaneously into diabodies, which were disassembled into monomers with an excess of the antibiotic trimethoprim (see picture).

Synthetic Methods

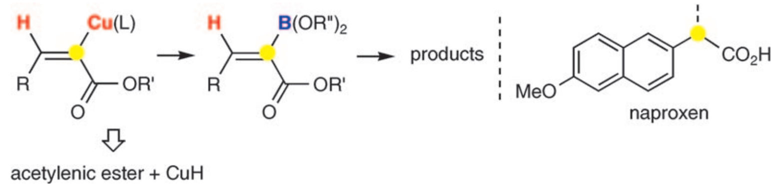

Stuck on an sp^2 carbon: A new route to geometrically defined α-alkoxycarbonyl-substituted vinylboronates consists of the chemo- and stereoselective 1,2-addition of copper hydride to acetylenic esters followed by stereoretentive transmetalation with pinacolborane. This strategy is applied to the generation of an aryl acrylate intermediate in the synthesis of the antiinflammatory drug naproxen (see scheme).

Asymmetric Domino Reactions

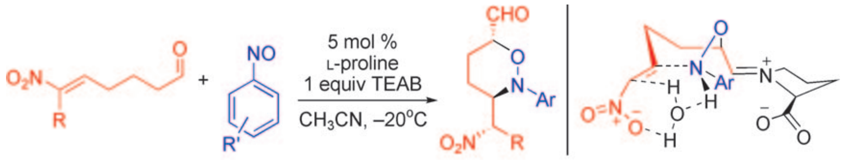

17 examples, up to 90% yield, >99% *ee*, >99:1 d.r.

Catalyst for THOught: The title reaction using acyclic nitroalkenals for the asymmetric installation of both C–O and C–N bonds led to functionalized tetrahydro-1,2-oxazines (THOs) having up to three stereogenic centers; the products were isolated in up to 90 % yield with excellent enantioselectivity and complete diastereoselectivity (see scheme). DFT calculations reveal an unprecedented transition state containing a molecule of water, which assists in the C–N bond-forming step by participating in two hydrogen bonds.

Protein–DNA Interactions

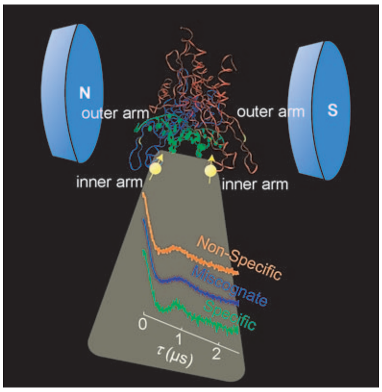

Constant embrace: Distance measurements obtained from pulsed electron spin resonance spectra show that the arms of *Eco*RI endonuclease occupy the same positions to enfold the DNA in specific, non-specific, and miscognate complexes.

Asymmetric Catalysis

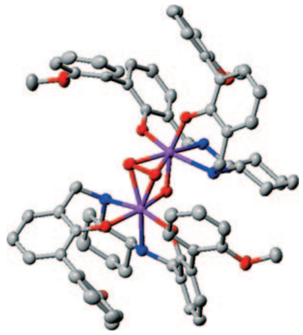

In the on-deck circle: A μ-oxo-μ-η^2:η^2-peroxo titanium(salan) complex (see structure; Ti purple, O red, N blue, C gray) was synthesized from the corresponding di-μ-oxo titanium(salan) complex using 30% hydrogen peroxide. The μ-oxo-μ-η^2:η^2-peroxo complex is slowly converted into an active species involved in the catalytic cycle of asymmetric epoxidation.

Supporting information is available on www.angewandte.org (see article for access details).

A video clip is available as Supporting Information on www.angewandte.org (see article for access details).

Service

Corrigendum

In this communication, the temperature used in monitoring the conversion of the *M* diastereomer into the *P* diasteromer was incorrectly quoted. On page 6124, right column, lines 11–12 from the top, it should read "After heating at 318 K", similarly in the caption to Figure 3 on the same page it should read "after heating in water solution at 318 K". The authors apologize for this error and wish to note that none of the interpretations in the paper are affected by this change.

Helicity Inversion in Lanthanide(III) Complexes with Chiral Nonaaza Macrocyclic Ligands

J. Gregoliński, J. Lisowski* _ **6122–6126**

Angew. Chem. Int. Ed. **2006**, *45*

DOI 10.1002/anie.200602464

Apology

During the preparation of the manuscript, a parallel report discussing a functionality variant of the presented transformation was inattentively left out, which should be included as reference [9d]. The authors of this Communication sincerely apologize for their oversight.

Organocatalytic Asymmetric α-Aminoxylation/Aza-Michael Reactions for the Synthesis of Functionalized Tetrahydro-1,2-oxazines

M. Lu, D. Zhu, Y. Lu, Y. Hou, B. Tan, G. Zhong* ______ **10187–10191**

Angew. Chem. Int. Ed. **2008**, *47*

DOI 10.1002/anie.200803731

---

[9] a) B. Tan, P. J. Chua, Y. Li, G. Zhong, *Org. Lett.* **2008**, *10*, 2437 – 2440; b) B. Tan, Z. Shi, P. J. Chua, G. Zhong, *Org. Lett.* **2008**, *10*, 3425 – 3428; c) B. Tan, P. J. Chua, X. Zeng, M. Lu, G. Zhong, *Org. Lett.* **2008**, *10*, 3489 – 3492; d) D. Zhu, M. Lu, P. J. Chua, B. Tan, F. Wang, X. Yang, G. Zhong, *Org. Lett.* **2008**, *10*, 4585 – 4588.